ELSEVIER

Journal of Structural Geology 26 (2004) 1127–1136

JOURNAL OF STRUCTURAL GEOLOGY

www.elsevier.com/locate/jsg

Controls on maximum fluid overpressure defining conditions for mesozonal mineralisation

Richard H. Sibson*

Department of Geology, University of Otago, PO Box 56, Dunedin, New Zealand

Received 27 November 2002; received in revised form 19 August 2003; accepted 2 September 2003

Abstract

The mesozonal environment for mineralisation ($\sim 10 \pm 5$ km depth) occurs towards the base of the seismogenic zone in the upper continental crust which, in areas of strong fluid release, acts as a stressed elastic lid containing overpressured hydrothermal fluids derived from metamorphic dehydration at depth. Au–quartz lodes in this environment are hosted by fault–fracture meshes comprising dilatant extensional and extensional-shear fractures interlinked by low-displacement faults. They form in a range of tectonic regimes but are most extensively developed in compressional/transpressional settings. A brittle failure mode plot contrasting compressional and extensional stress regimes demonstrates that: (i) high fluid overpressures are easier to sustain in compressional regimes that also allow the highest amplitude fluid-pressure cycling; (ii) dilatant mesh structures serve as high-permeability conduits only under high fluid-pressure and low differential stress in the absence of through-going cohesionless faults that are well-oriented for reactivation; and, (iii) the critical interdependence of differential stress and sustainable overpressure ensures that changes in stress state are accompanied by fluid redistribution. The specialised circumstances allowing high-flux flow of overpressured fluids are generally short-lived and are terminated by the formation of through-going, favourably oriented faults.

Keywords: Mesozonal gold; Faults; Fractures; Stress; Fluid-pressure

1. Introduction

Mesozonal Au–quartz lodes occupy fault–fracture meshes developed in association with shear zones of mixed brittle–ductile character active within a sub-greenschist to mid-greenschist metamorphic environment ($200 < P < 400$ MPa and $250 < T < 400$ °C) (Ho, 1987; Roberts, 1987; Sibson and Scott, 1998). Their inferred depth range of ~7–14 km corresponds loosely with the lower half of the continental seismogenic zone whose base is controlled by isotherms at ~350 and ~450 °C, respectively, for quartz- and feldspar-dominant lithologies (Sibson, 1984; Scholz, 1988; Ito, 1999). Though known from a variety of tectonic settings, the lode systems generally attain their greatest development in compressional/transpressional regimes (Kerrich and Wyman, 1990).

Estimates of gold and quartz solubilities for the appropriate hydrothermal conditions suggest that formation of such vein systems involves the passage of large fluid volumes. For example, flow of ~1 km^3 of hydrothermal fluid could potentially give rise to a modest deposit containing ~10 tonnes of Au housed in a quartz ore-shoot occupying ~4×10^5 m^3 (e.g. a 1 m × 400 m × 1000 m vein) carrying 10 g/tonne (Seward, 1993). Vein textures generally imply, however, that focused flow through hosting fault–fracture systems was intermittent, involving multiple episodes of hydrothermal transport and deposition. In addition, investigations of microstructures in extension veins within the meshes reveal evidence of open-space filling in some instances (Boullier and Robert, 1992; Cox, 1995).

Given the evidence for high-flux focused flow through mesh structures with gaping fractures, the specific question addressed by this paper is the problem of void creation in the mesozonal environment where overburden pressures are of the order of 260 MPa (equivalent to ~26,000 tonnes/m^2). The need for near-lithostatic values of fluid-pressure to offset the overburden pressure and create void-space in such environments has long been recognised (e.g. Etheridge, 1983; Cox et al., 1991). Here, the specific structural conditions under which such overpressures may develop

* Tel.: +64-3-479-7506; fax: +64-3-479-7527.
E-mail address: rick.sibson@stonebow.otago.ac.nz (R.H. Sibson).

0191-8141/$ - see front matter © 2004 Elsevier Ltd. All rights reserved.
doi:10.1016/j.jsg.2003.11.003

and be sustained are defined. The restricted circumstances under which this may occur have direct implications for exploration in the mesozonal environment.

2. Structural setting for mesozonal mineralisation

2.1. The seismogenic zone as an upper crustal stress guide

Strength profiles of the crust constructed for regions undergoing prograde metamorphism with associated fluid release at depth suggest that fault strength attains a maximum between the middle and the base of the frictional seismogenic zone and diminishes to very low values beneath it as fluid-pressures approach lithostatic (Sibson and Scott, 1998). In such regions the sub-greenschist carapace serves as the principal load-bearing portion of the crust, acting as an upper crustal stress guide (Fig. 1). Support for this concept of the hydrostatically pressured portion of the upper crust as the principal load-bearing component of the lithosphere comes from analyses of deep borehole stress measurements in cratonic areas and modern reassessments of continental earthquake depth distribution (Zoback and Townend, 2001; Jackson, 2002).

Measurements of present-day tectonic stress fields (principal compressive stresses $\sigma_1 > \sigma_2 > \sigma_3$) across the Earth also demonstrate the existence of remarkably uniform 'Andersonian' stress provinces over broad areas, with two of the principal stresses horizontal and the vertical stress, σ_v, either equal to σ_1 (extensional regime), σ_3 (compressional regime), or σ_2 (strike-slip regime) (Anderson, 1951; Zoback, 1992). Transitions between simple 'Andersonian' stress states must, however, occur at the boundaries between stress provinces. Local stress heterogeneity may also result, for example, through local buckling or torsion of the 'elastic lid'. It is important to keep these possibilities in mind throughout the following discussion, which focuses on the effects of simple 'Andersonian' stress fields (where stress trajectories are either horizontal or vertical) on the containment of overpressured fluids.

2.2. Hosting fault–fracture meshes

Mesozonal Au–quartz veins are commonly hosted within fault–fracture meshes that comprise various combinations of extension and extensional-shear fractures interlinked by low-displacement shears (Fig. 2). Note that the style of fault–fracture meshes varies considerably, a key factor being the proportion and distribution of relatively high competence (i.e. high tensile strength) rock that promotes extensional over shear failure (Sibson, 1996, 2000). The distributed fault–fracture meshes are often transected, at a late stage in their development, by throughgoing, optimally oriented faults. Though described from a range of tectonic settings (e.g. Ames, 1948; Robert and Brown, 1986; Cox et al., 1991; Craw and Norris, 1991; Miller et al., 1992; Robert et al., 1995; Nguyen et al., 1998), the lode systems typically reach their greatest development in compressional/transpressional regimes where they are commonly associated with reverse faults that, demonstrably, were *severely misoriented* for frictional reactivation in the prevailing stress field at the time of mineralisation (Sibson et al., 1988). In the extension and extensional-shear veins, growth textures commonly record a history of incremental 'crack-seal' dilatation (Ramsay, 1980) with occasional evidence for episodes of open-space filling (Boullier and Robert, 1992), suggesting that the hosting fractures were locally gaping at the time of hydrothermal flow and deposition. Fault-veins often exhibit ribbon texture with bands of quartz interlaminated with slivers of detached wallrock developed subparallel to the walls. From a structural–hydrological perspective, it seems clear that the

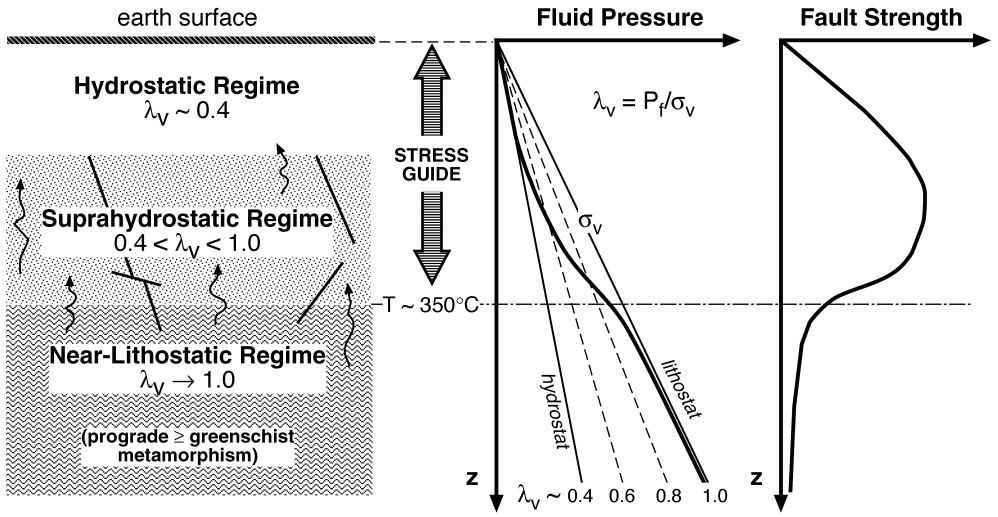

Fig. 1. Hypothetical fluid-pressure profile through the carapace to a region undergoing prograde metamorphism defining the seismogenic zone ($T < 350$ °C) as an upper crustal stress guide. Pore-fluid factor, $\lambda_v = P_f/\sigma_v$ defines fluid-pressure level at different depths.

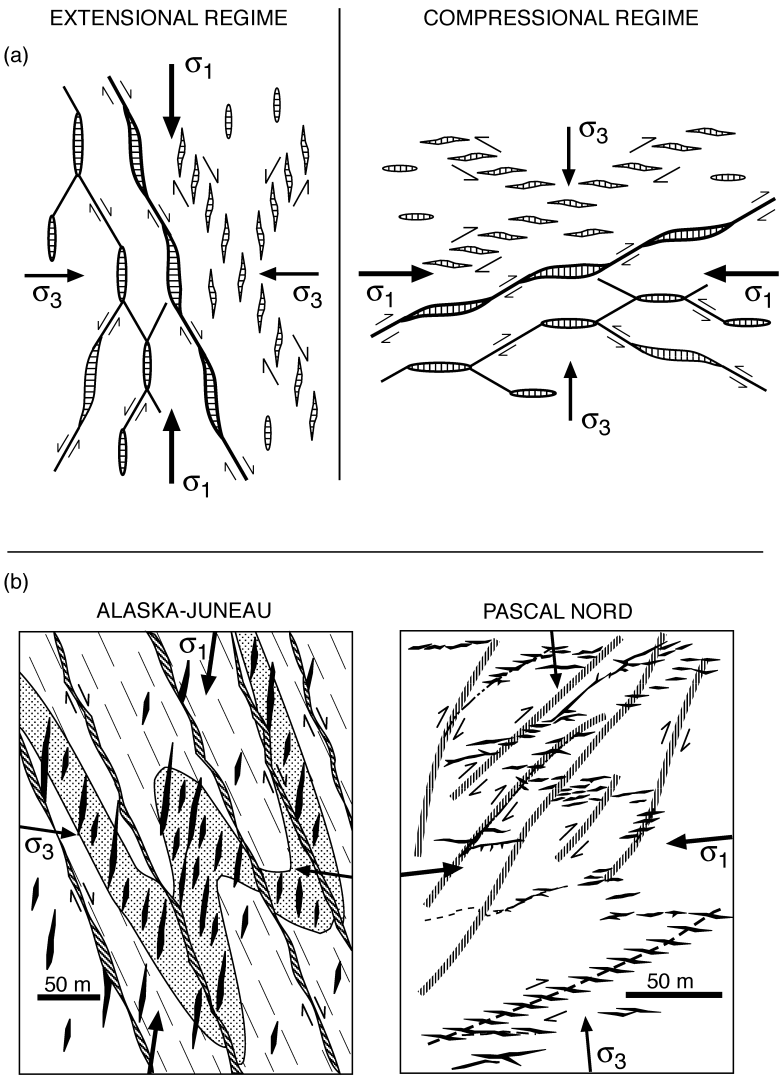

Fig. 2. Fault–fracture meshes in extensional and compressional regimes: (a) hypothetical examples showing variations in mesh style and incipient linkage of different components (bold) to form a through-going fault; (b) cartoons of mesozonal lode systems hosted in fault–fracture meshes—the extensional Alaska–Juneau lode system comprising fault-veins (diagonal cross-hatching) developed along a system of normal faults interlinked by extension veins (black) preferentially concentrated within a high competence folded gabbro layer set in a cleaved pelitic matrix (after Miller et al., 1992), and the compressional fault–fracture mesh of the Pascal Nord (formerly Perron) Mine, Quebec, where extension veins (black) in semi-brittle shear zone arrays with incipient through-going faults are developed in the vicinity of moderate-to-steeply dipping reverse-sense ductile shear zones (thick diagonally hatched lines) (after Ames, 1948).

fault–fracture meshes functioned as localised high-permeability conduits within otherwise low-permeability crust, allowing episodic rapid flow of substantial fluid volumes.

3. Brittle failure controls on maximum overpressure

3.1. Fluid pressure and effective stress in the crust

In a rock mass where pore and fracture space is fluid-saturated and interconnected, the general law of effective stress (Rice and Cleary, 1976) states that all normal stresses acting on planes, σ_n, are reduced to effective values

$$\sigma'_n = (\sigma_n - \alpha P_f) \quad (1)$$

where the poroelastic parameter, α, generally approaches unity. On the assumption that $\alpha = 1$, this gives rise to the simplified law where the effective principal compressive stresses are

$$\sigma'_1 = (\sigma_1 - P_f) > \sigma'_2 = (\sigma_2 - P_f) > \sigma'_3 = (\sigma_3 - P_f) \quad (2)$$

(Terzaghi, 1943). At depth, z, within the crust, the fluid pressure state may be defined in relation to the overburden pressure or vertical stress, σ_v, by the pore-fluid factor

$$\lambda_v = \frac{P_f}{\sigma_v} = \frac{P_f}{\varrho g z} \quad (3)$$

where ϱ is average rock density and g is the gravitational acceleration (Hubbert and Rubey, 1959). The effective

vertical stress is then

$$\sigma'_v = (\sigma_v - P_f) = \varrho g z(1 - \lambda_v) \quad (4)$$

so that the effects of confining overburden pressure are progressively reduced as $\lambda_v \rightarrow 1$.

When pore space, cracks, and fractures are saturated with fluid of density, ϱ_f, interconnected to a water table at the Earth's surface, the fluid pressure state is hydrostatic with $P_f = \varrho_f g z$, so that $\lambda_v = \varrho_f/\varrho \sim 0.4$ for aqueous fluid and a rock density, $\varrho \sim 2650\ \mathrm{kg/m^3}$. Overpressuring above hydrostatic values (i.e. $\lambda_v > 0.4$) occurs in areas of rapid fluid release or generation within the crust where drainage is impeded by low-permeability layering (Neuzil, 1995). Such areas include compacting sedimentary basins (Osborne and Swarbrick, 1997), deforming fore-arc accretionary prisms (Moore and Vrolijk, 1992), regions undergoing prograde metamorphism (Etheridge et al., 1984), and areas where magma is actively intruding fluid-saturated rocks (Fournier, 1999). In all such settings, overpressures may approach or possibly even exceed lithostatic values ($\lambda_v \rightarrow 1.0$) at depth.

3.2. Brittle failure criteria

In empirical 'engineering' rock mechanics, three macroscopic modes of brittle failure, all dependent on fluid-pressure, are recognised within intact isotropic rock and may be used to construct a composite failure envelope on a Mohr diagram (Fig. 3) defining the relationship between shear stress, τ, and effective normal stress, $\sigma'_n = (\sigma_n - P_f)$, on potential failure planes (Brace, 1960; Secor, 1965; Jaeger and Cook, 1979). When $\sigma'_n > 0$, faults form by compressional shear failure in accordance with the linear Coulomb criterion

$$\tau = C + \mu_i \sigma'_n \approx 2T + \mu_i(\sigma_n - P_f) \quad (5)$$

where $C \sim 2T$ is the cohesive strength of the rock, and μ_i is the coefficient of internal friction which, for most rocks, lies in the range $0.5 < \mu_i < 1.0$ (Jaeger and Cook, 1979); in Fig. 3 and hereafter, we adopt a representative value, $\mu_i = 0.75$. Faults tend to form along planes containing the σ_2 direction at angles $\theta_i = 0.5\tan^{-1}(1/\mu_i)$ to the σ_1 direction (typically $25° < \theta_i < 30°$). In the tensile field ($\sigma'_n < 0$), failure is governed by the macroscopic Griffith criterion of parabolic form

$$\tau^2 = 4(\sigma_n - P_f)T + 4T^2 \quad (6)$$

which describes the stress conditions for extensional shear failure along planes oriented at $\theta < \theta_i$ to σ_1 when $\sigma'_n < 0$. For zero shear stress this expression reduces to the hydraulic fracture criterion

$$\sigma'_3 = -T \qquad \text{or} \qquad P_f = \sigma_3 + T \quad (7)$$

describing conditions for the formation of pure extension fractures perpendicular to σ_3. The type of failure that occurs within intact rock depends on the ratio of differential stress, $(\sigma_1 - \sigma_3)$, to tensile strength, T: for $\mu_i = 0.75$, compressional shear failure occurs when $(\sigma_1 - \sigma_3) > 5.66T$, extensional-shear requires $5.66T > (\sigma_1 - \sigma_3) > 4T$, and hydraulic extension fracturing requires $(\sigma_1 - \sigma_3) < 4T$ (Secor, 1965). In the case of existing cohesionless faults, the condition for reshear is

$$\tau = \mu_s \sigma'_n = \mu_s(\sigma_n - P_f) \quad (8)$$

where μ_s is the coefficient of static friction (Jaeger and Cook, 1979). A value $\mu_s = 0.6$ is adopted throughout the

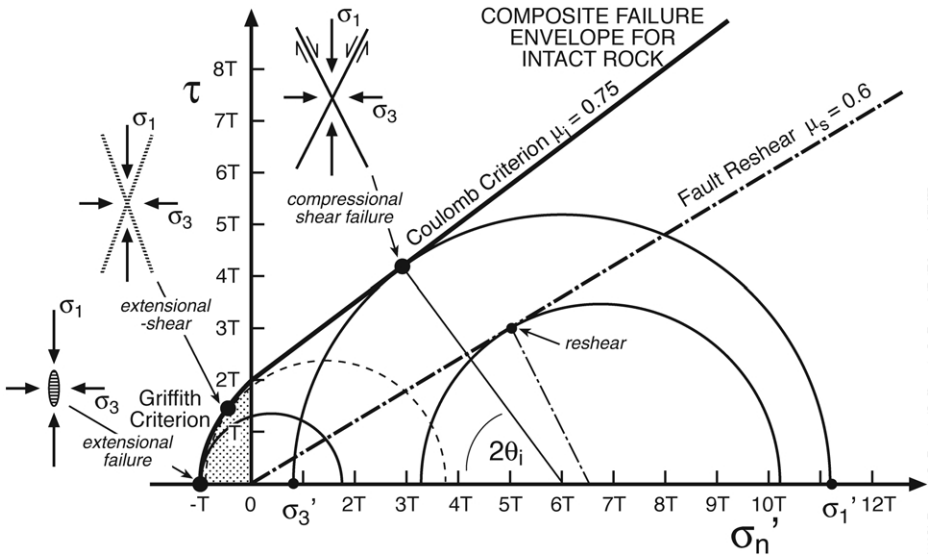

Fig. 3. Composite failure envelope for intact rock (bold line) plus the reshear condition for a cohesionless fault (dash–dot line) plotted on a Mohr diagram of shear stress, τ, against effective normal stress, σ'_n, normalised to rock tensile strength, T. Critical stress circles are shown for the three macroscopic modes of brittle failure and for the reshear of an optimally oriented cohesionless fault. Expected orientations with respect to the principal stress axes of new-formed compressional shear, extensional-shear, and extension fractures are shown in the attached cartoons.

following analysis (Fig. 3), near the bottom of the experimental range for rock friction (Byerlee, 1978) but consistent with $\mu_i = 0.75$ (Lockner and Byerlee, 1993).

3.3. Comparative failure mode plot

On the assumption of 'Andersonian' stress regimes with one principal stress, σ_v, vertical and the others lying in a horizontal plane ($\sigma_H > \sigma_h$), the composite failure envelopes for intact rock derived from these failure criteria (Eqs. (5)–(7) defining the different modes of macroscopic failure), together with the reshear condition (Eq. (8)) may be transposed to plots of differential stress ($\sigma_1 - \sigma_3$) versus effective vertical stress, $\sigma'_v = (\sigma_v - P_f)$ (Sibson, 1998, 2000). In turn (from Eq. (4)) this allows the failure conditions to be defined on plots of ($\sigma_1 - \sigma_3$) versus λ_v, the pore-fluid factor, for a given depth. Fig. 4 is an example of such a plot constructed for the mesozonal environment at 10 km depth for both compressional ($\sigma_v = \sigma_3$) and extensional ($\sigma_v = \sigma_1$) regimes. The layout of the figure is designed to contrast the failure conditions during crustal extension and compression, and to emphasize the effects to be expected from transitions between the two stress regimes as may occur during coaxial tectonic inversion (Williams et al., 1989). Note that failure curves for a strike-slip regime ($\sigma_v = \sigma_2$) have intermediate values bounded by the compressional and extensional regime criteria, depending on the precise value of σ_2 between σ_1 and σ_3.

The failure envelopes for intact rock are normalised to rock tensile strength which, from Lockner's (1995) compilation, ranges from 1 to 10 MPa for most sedimentary rocks to values approaching or exceeding 20 MPa for some crystalline rocks. The solid lines define composite failure envelopes for intact rock with $T = 5$, 10, 15 and 20 MPa; along each curve there is a transition from extensional (ext) through extensional-shear (es) to compressional shear failure (cs) as differential stress increases. Dash–dot lines define the reshear condition for optimally oriented cohesionless faults (i.e. faults containing the σ_2 axis and oriented at $\sim 30^\circ$ to the σ_1 direction).

3.4. Controls on maximum overpressure

Formation of new brittle fractures or faults, or reshear of existing faults, may all create drainage paths through caprocks to overpressured crust, thereby limiting the degree of overpressuring Fig. 4 defines the stress/fluid-pressure conditions at 10 km depth for different types of brittle failure or reshear, and can thus be used to define the limits to overpressure under 'Andersonian' stress regimes in the

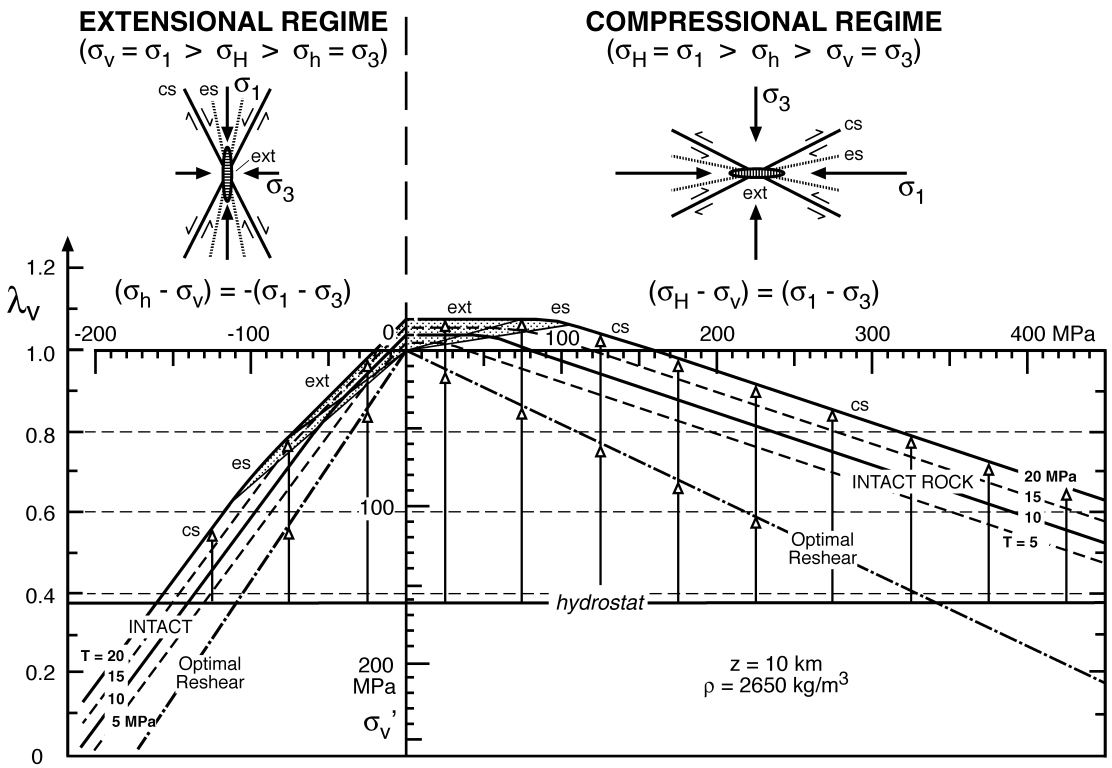

Fig. 4. Brittle failure mode plot of differential stress ($\sigma_1 - \sigma_3$) versus the pore-fluid factor, $\lambda_v = P_f/\sigma_v$, (and effective vertical stress, σ'_v) at 10 km depth, defining maximum sustainable overpressure for compressional and extensional tectonic regimes. Failure envelopes for intact rock are constructed for internal friction, $\mu_i = 0.75$ and $T = 5$, 10, 15 and 20 MPa (cs, es, and ext define fields of compressional shear, extensional-shear, and extensional failure); reshear of optimally oriented faults assumes static friction, $\mu_s = 0.6$; rock density, $\varrho = 2650$ kg/m^3. Shaded areas define fields where mesh structures incorporating gaping extension and extensional-shear fractures may develop. Hydrostatic fluid-pressure condition represented by bold line at $\lambda_v = 0.38$; vertical open-headed arrows represent sustainable overpressure above hydrostatic at particular values of differential stress for intact rock ($T = 20$ MPa), and for reshear.

mesozonal environment. Vertical open-headed arrows extending above the hydrostat at particular values of differential stress define the maximum sustainable overpressure before brittle failure or fault reshear occurs in either compressional or extensional tectonic regimes. Major implications are

1. Fluid overpressures are clearly easier to maintain in compressional tectonic regimes. Maximum sustainable overpressure decreases with increasing differential stress in both compressional and extensional regimes, but the fall-off occurs a great deal more rapidly in crust under extension. Geometrical considerations reinforce these mechanical controls on overpressure: subvertical extension fractures and steeply dipping normal faults promote high vertical permeability in extensional regimes, contrasting with subhorizontal extension fractures and low dipping thrusts in compressional regimes (Fig. 4). It is also evident that the potential for high amplitude fluid-pressure cycling from fault-valve action (Sibson et al., 1988) is far greater in compressional regimes. This is important for mineralisation because the drop in fluid pressure (ΔP_f) accompanying discharge through mesh structures across steep hydraulic gradients is likely to be a major factor contributing to hydrothermal precipitation (Cox et al., 1991; Cox, 1995; Wilkinson and Johnston, 1996; Parry, 1998). Evidence for large amplitude ($\sim$lithostatic-to-hydrostatic) fluid-pressure fluctuations has in fact been found in fluid inclusion studies on fault–fracture vein meshes associated with steep reverse faults (Robert et al., 1995).
2. The presence of through-going low-cohesion faults that are optimally oriented for frictional reactivation in the prevailing stress field inhibits all modes of brittle failure within intact rock and provides a lower bound to maximum overpressure for a given differential stress state. Relevant here is the demonstration by Barton et al. (1995) that the greatest hydraulic conductivity within multiple fracture sets tends to occur along fractures that are favourably oriented for reshear in the prevailing stress field. Note, however, that extension and extensional-shear fractures may also develop around faults that are *severely misoriented* for reactivation in the prevailing tectonic stress field (Sibson et al., 1988). Faults containing the σ_2 axis and possessing frictional coefficients in Byerlee's (1978) experimental range, $0.6 < \mu_s < 0.85$, become severely misoriented for frictional reactivation when they lie at >50–60° to σ_1.
3. Formation of extension and extensional-shear fractures is only possible at comparatively low values of differential stress ($(\sigma_1-\sigma_3) < 5.66T$—shaded areas in Fig. 4) (Secor, 1965; Etheridge, 1983). In compressional regimes their development requires supralithostatic levels of fluid-pressure (i.e. $\lambda_v > 1.0$) unless stress heterogeneity exists such that $\sigma_3 < \sigma_v$.

3.5. Conditions for high-flux flow and lode formation

Within fault–fracture meshes hosting mesozonal Au–quartz lodes, the widespread distribution of extension and extensional-shear veins with crack-seal and open-space fill textures suggests local attainment of the *tensile overpressure condition*, $P_f > \sigma_3$, allowing flow through gaping fractures. The shaded portions of Fig. 4 therefore define the restricted stress/fluid-pressure conditions under which gaping fractures can be maintained in fault–fracture meshes, allowing high-flux flow to accompany fault-valve action. The greater the tensile strength, the greater the range of differential stress under which high-flux flow may occur.

Note that there is also a general tendency for rock permeability to increase as $P_f \rightarrow \sigma_3$ and $\sigma_3' \rightarrow 0$, increasing flow-rate for a given head gradient even when conditions for macroscopic brittle fracturing are unachieved (Seront et al., 1998; Cox et al., 2001). Such enhancement of permeability at high fluid-pressure ($\lambda_v \rightarrow 1$) and low differential stress may be especially important in shear zones acting as localised fluid conduits.

4. Tectonic settings allowing maximum overpressure

The shaded portions of the brittle failure mode plot in Fig. 4 define the restricted set of stress/fluid-pressure conditions under which fault–fracture meshes become dilatant in compressional and extensional regimes. The presence of high tensile strength material expands the range of differential stress under which dilatancy and high-flux flow may occur. Another important requirement is an absence of low-cohesion, through-going faults that are well-oriented for reshear in the prevailing stress field (Sibson, 2000). Together, these criteria may be used to define likely tectonic settings for development of mesozonal Au–quartz lodes which, in general, must be fluid-rich overpressured environments under comparatively low differential stress.

4.1. Intact or reconstituted crust

In at least its uppermost levels, the bulk permeability of mature crystalline crust is so high from pervasive fracturing that it seems incapable of confining overpressured fluid over significant time periods (Townend and Zoback, 2000) Crust freshly reconstituted by metamorphism, however, will initially have negligible fracture permeability. In particular, the base of a progressively cooling and thickening carapace to a belt of prograde regional metamorphism may act as a low-permeability caprock to overpressured metamorphic fluids. For example, mesozonal vein swarms hosted predominantly by extensional fault–fracture meshes within the Otago Schist belt, New Zealand, seem to have been 'self-generated' in essentially intact crust by migrating late-metamorphic fluids (Craw and Norris, 1991; Sibson and Scott, 1998).

4.2. Faults with restored cohesive strength

Fault–fracture meshes can develop and continue to be reactivated in the vicinity of faults that are well-oriented for reshear, provided they have regained cohesive strength approaching that of intact rock through hydrothermal cementation and allied processes. For example, in the Revenge gold mine, Kambalda, Western Australia, lode systems are hosted in fault–fracture meshes developed around well-oriented thrust faults that have undergone multiple episodes of cementation (Nguyen et al., 1998). Reshearing is commonly localised at the contact between the fault-hosted vein and the wallrock. Continued reactivation and dilation of such mesh structures can only occur, however, so long as fault cohesive strength is restored between successive failure episodes.

4.3. Faults misoriented from inheritance

Dilatant fault–fracture meshes may also develop around faults that are severely misoriented for reactivation in the prevailing tectonic stress field (i e. oriented to σ_1 at greater than the frictional lock-up angle) (Sibson et al., 1988). Under appropriate fluid-pressure conditions this may occur where fault sets inherited from a previous tectonic regime are loaded in the active stress state. An obvious example is that of coaxial compressional inversion where steep normal faults developed within fluid-rich sedimentary basins during crustal extension subsequently become loaded as steep reverse faults under horizontal compression (Fig. 5a). The increase in mean stress accompanying such a transition may help elevate fluid-pressure leading to dilatant mesh development (Sibson, 1995).

4.4. Progressive rotational misorientation of faults

Sets of faults developed initially at favourable orientations within a stress regime may undergo 'domino rotation' (Fig 5b) with progressive deformation to frictional lock-up. In overpressured environments, mesh structure may then develop as the faults enter the field of severe misorientation (orientation at >50–60° to σ_1). Progressive steepening of initially low-angle thrusts towards the rear of accretion–collision complexes in the fore-arc hanging walls of subduction zones provides a particularly favourable compressional environment for mesh activation (Fig. 6a), with abundant fluids derived from the accretionary complex and from dehydration of subducting oceanic lithosphere (Peacock, 1990; Moore and Vrolijk, 1992). This is the likely setting for mesozonal mineralisation associated with steep reverse faults in the Mother Lode gold belt in the Sierra Nevada foothills of California and in comparable Archean environments (Kerrich and Wyman, 1990). Horizontal contraction in such settings may also involve tightening and amplification of steep-to-upright folds with mesh development linked to reverse slip along steepening fold limbs as well as progressively steepening thrusts. Au–quartz mineralisation developed within fault–fracture meshes associated with both fold hinges and reverse-faults is well displayed in the Paleozoic Lachlan fold-belt of SE

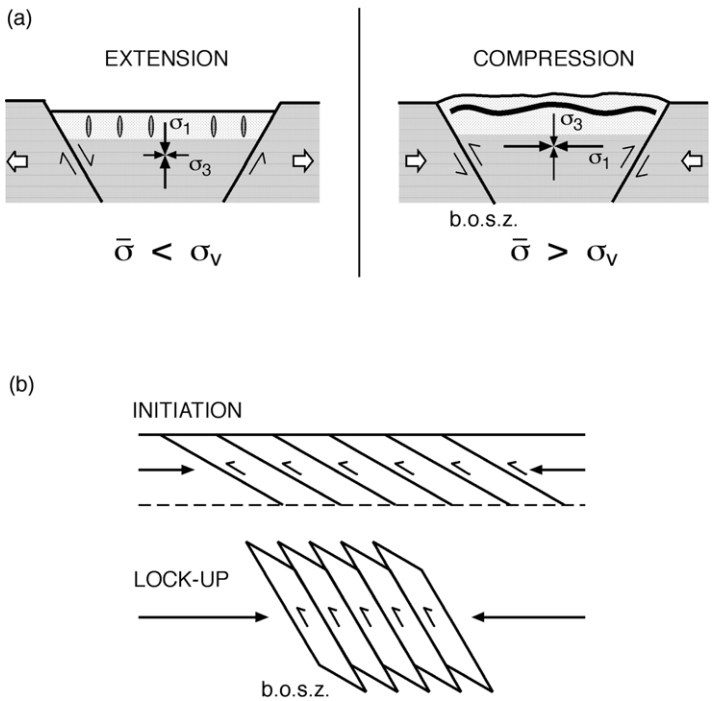

Fig. 5. Fluid-rich contractional tectonic settings for high-flux flow through fault-fracture meshes developed near the base of the seismogenic zone (b.o.s.z.): (a) compressional inversion of a sedimentary basin in rifted crust; (b) domino-steepening of reverse faults during progressive shortening in an accretion–collision belt.

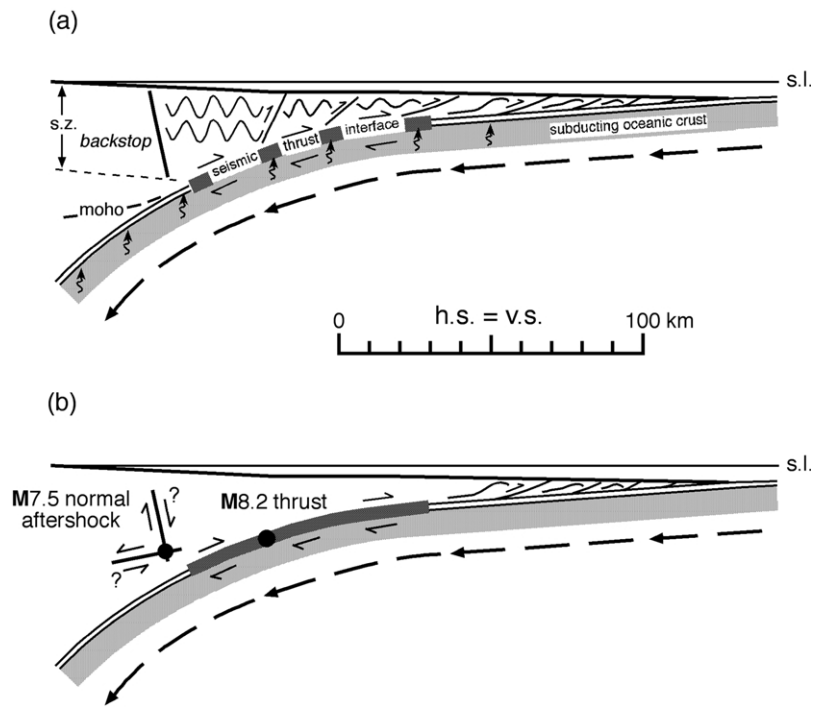

Fig. 6. Schematic cartoons of deformation in subduction hanging-walls. (a) Steepening of reverse faults and fold tightening towards subduction backstop near rear of fore-arc (s.z. = fore-arc seismogenic zone). (b) The 1968 Tokachi–Oki earthquake sequence in northern Japan (after Magee and Zoback, 1993): an M8.2 thrust rupture along the subduction interface followed by an M7.5 normal-slip rupture in the landward hanging wall. It is uncertain on which focal planes the M7.5 normal-slip rupture occurred, though Magee and Zoback (1993) favoured the low-dipping plane.

Australia (Cox et al., 1991; Cox, 1995; Gray, 1997; Sibson and Scott, 1998; Schaubs and Wilson, 2002).

4.5. Effects of changes in the stress state

Fig 4 illustrates the critical interdependence of maximum overpressure and differential stress in compressional and extensional tectonic regimes. Interesting scenarios for fluid redistribution arise during transitions between the two stress regimes, especially when they take place over short time periods. As discussed, a coaxial transition from an extensional to a compressional stress regime (compressional inversion) is accompanied by an increase in maximum sustainable overpressure and also by an increase in mean stress that may act to boost fluid-pressure (Sibson, 1995). Provided the region remains devoid of faults well-oriented for reshear, this provides a suitable environment for generation of dilatant fault–fracture meshes.

In contrast, a progressive change from a compressional regime to an extensional regime (negative inversion) leads initially to an increase in sustainable overpressure (so long as $\sigma_1 > \sigma_v$), and then to an abrupt reduction in sustainable overpressure once the stress axes switch and $\sigma_v = \sigma_1$. Massive fluid loss may then occur through 'self-generation' of vertical extension fractures and normal faults in an extensional mesh. This is the origin postulated for the Alaska–Juneau Au–quartz lode system hosted by an extensional fault–fracture mesh (Fig. 2) within an otherwise progressively contracting Eocene fore-arc environment (Miller et al., 1992; Sibson and Scott, 1998). Note that seismological evidence suggests that switches in the local stress regime sometimes occur almost instantaneously in subduction settings. Fig. 6 illustrates the 1968 M8.2 Tokach-oki subduction thrust rupture in Japan, which was followed by a major M7.5 normal-slip aftershock towards the rear of the fore-arc (Kanamori, 1971; Magee and Zoback, 1993). Though it is unclear which plane from the focal mechanism was responsible for the aftershock (Fig. 6b), it is apparent that the stress-drop accompanying thrusting changed the crustal stress-state throughout a huge volume of rock near the down-dip termination of the thrust rupture, creating a setting for fluid-release akin to that inferred for the Alaska–Juneau deposit. On seismological evidence, Husen and Kissling (2001) inferred a similar episode of massive fluid release following a large subduction thrust rupture.

5. Discussion

The key to understanding mesozonal Au–quartz lodes involves defining the tectonic conditions that allow the accumulation and containment of fluids overpressured to near-lithostatic values in the mid-crust, and their intermittent release through fault-valve action. The level of overpressure that can accumulate depends on the tectonic setting, the localised stress state, and inherited brittle architecture (Sibson and Scott, 1998). Brittle failure mode

plots (Fig. 4) demonstrate that the overpressure conditions required for lode formation can only develop in extremely restricted circumstances, a key factor being the absence of through-going low-cohesion faults that are well-oriented for reshear. Thus, the specialised conditions for maintaining dilatant fault–fracture meshes allowing high-flux flow are likely to be short-lived and, on the field evidence, are frequently terminated by the formation of new through-going, favourably oriented faults.

High overpressures are easiest to sustain in compressional tectonic regimes that also have the potential for the highest amplitude cycling of fluid-pressure (ΔP_f) through fault-valve action. Development of mesozonal mineralisation within fault-fracture meshes in the mesozonal environment is most likely in fluid-rich environments such as the forearc hanging walls of subduction zones and during compressional inversion. Significant fluid redistribution may also be induced by changes in the regional stress state in areas of overpressuring.

The tectonic settings for high-flux flow in the mesozonal environment are easily translated into exploration criteria but in areas of polyphase deformation it is important to separate out stress-controlled syn-mineralisation structures from pre- and post-mineralisation structures. Subsequent overprinting may obscure the relationship of hosting structures to the tectonic stress field at the time of mineralisation.

Acknowledgements

Thanks first to Neville Price for starting me on the path of fluid–fault interactions. Many of the concepts developed here evolved from discussions over many years with Graeme Broadbent, Stephen Cox, Dave Craw, Lance Miller, Howard Poulsen and Francois Robert, together with postgraduate researchers John Scott and Mike Begbie. I thank the organisers of *Applied Structural Geology for Mineral Exploration and Mining* for the opportunity to participate in the KAL2002 International Symposium, and reviewers Jamie Connolly and Titus Murray for constructive comments.

References

Ames, H.G., 1948. The Perron mine. In: Structural Geology of Canadian Ore Deposits. Canadian Institute of Mining and Metallurgy, pp. 893–898.

Anderson, E.M., 1951. The Dynamics of Faulting and Dyke Formation with Application to Britain, 2nd ed, Oliver and Boyd, Edinburgh.

Barton, C.A., Zoback, M.D., Moos, D., 1995. Fluid flow along potentially active faults in crystalline rock. Geology 23, 683–686.

Boullier, A.-M., Robert, F., 1992. Paleoseismic events recorded in Archean gold–quartz vein networks, Val d'Or, Abitibi, Quebec, Canada. Journal of Structural Geology 14, 161–180.

Brace, W.F., 1960. An extension of the Griffith theory of fracture to rocks. Journal of Geophysical Research 65, 3477–3480.

Byerlee, J.D., 1978. Friction of rocks. Pure and Applied Geophysics 116, 615–626.

Cox, S.F., 1995. Faulting processes at high fluid pressures: an example of fault-valve behaviour from the Wattle Gully Fault, Victoria, Australia. Journal of Geophysical Research 100, 12,841–12,860.

Cox, S.F., Wall, V.J., Etheridge, M.A., Potter, T.F., 1991. Deformation and metamorphic processes in the formation of mesothermal vein-hosted gold deposits—examples from the Lachlan Fold Belt in central Victoria, Australia. Ore Geology Reviews 6, 391–423.

Cox, S.F., Knackstedt, M.A., Braun, J., 2001. Principles of structural control on permeability and fluid flow in hydrothermal systems. Reviews in Economic Geology 14, 1–24.

Craw, D., Norris, R.J., 1991. Metamorphogenic Au–W veins and regional tectonics: mineralisation throughout the uplift history of the Haast Schist, New Zealand. New Zealand Journal of Geology and Geophysics 34, 373–383.

Etheridge, M.A., 1983. Differential stress magnitudes during regional deformation and metamorphism: upper bound imposed by tensile fracturing. Geology 11, 231–234.

Etheridge, M.A., Wall, V.J., Cox, S.F., Vernon, R.H., 1984. High fluid pressures during regional metamorphism and deformation: implications for mass transport and deformation mechanisms. Journal of Geophysical Research 89, 4344–4358.

Fournier, R.O., 1999. Hydrothermal processes related to movement of fluid from plastic into brittle rock in the magmatic–epithermal environment. Economic Geology 94, 1193–1211.

Gray, D.R., 1997. Tectonics of the southeastern Australian Lachlan Fold Belt: structural and thermal aspects. In: Burg, J.-P., Ford, M. (Eds.), Orogeny Through Time. Geological Society Special Publication 121, pp. 149–177.

Ho, S.E., 1987. Fluid inclusions: their potential as an exploration tool for Archean lode gold deposits. In: Ho, S.E., Groves, D.I. (Eds.), Recent Advances in Understanding Precambrian Gold Deposits, Vol. 1. University of Western Australia Geology Department Publication 11, pp. 239–264.

Hubbert, M.K., Rubey, W.W., 1959. Role of fluid pressure in mechanics of overthrust faulting. Bulletin of the Geological Society of America 70, 115–166.

Husen, S., Kissling, E., 2001. Postseismic fluid flow after the large subduction earthquake of Antofagasta, Chile. Geology 29, 847–850.

Ito, K., 1999. Seismogenic layer, reflective lower crust, surface heat flow and large inland earthquakes. Tectonophysics 306, 423–433.

Jackson, J., 2002. Strength of the continental lithosphere: time to abandon the jelly sandwich. GSA Today 12, 4–10.

Jaeger, J.C., Cook, N.G.W., 1979. Fundamentals of Rock Mechanics, 3rd ed, Chapman and Hall, London.

Kanamori, H., 1971. Focal mechanism of the Tokachi–Oki earthquake of May 16, 1968: contortion of the lithosphere at a junction of two trenches. Tectonophysics 12, 1–13.

Kerrich, R., Wyman, D., 1990. Geodynamic setting of mesothermal gold deposits: an association with accretionary tectonic regimes. Geology 18, 882–885.

Lockner, D.A., 1995. Rock failure. In: Ahrens, T.J. (Ed.), Rock Physics and Phase Relations: a Handbook of Physical Constants. American Geophysical Union Reference Shelf, 3, pp. 127–147.

Lockner, D.A., Byerlee, J.D., 1993. How geometrical constraints contribute to the weakness of mature faults. Nature 363, 250–252.

Magee, M.E., Zoback, M.D., 1993. Evidence for a weak interplate thrust fault along the northern Japan subduction zone and implications for the mechanics of thrust faulting and fluid expulsion. Geology 21, 809–812.

Miller, L.D., Barton, C.C., Fredericksen, R.S., Bressler, J.R., 1992. Structural evolution of the Alaska–Juneau gold deposit, southeastern Alaska. Canadian Journal of Earth Science 29, 865–878.

Moore, J.C., Vrolijk, P., 1992. Fluids in accretionary prisms. Reviews of Geophysics 30, 113–135.

Neuzil, C.E., 1995. Abnormal pressures as hydrodynamic phenomena. American Journal of Science 295, 742–786.

Nguyen, P.T., Cox, S.F., Harris, L.B., Powell, C.M., 1998. Fault-valve behaviour in optimally oriented shear zones: an example at the Revenge gold mine, Kambalda, Western Australia. Journal of Structural Geology 20, 1625–1640.

Osborne, M.J., Swarbrick, R.E., 1997. Mechanisms for generating overpressure in sedimentary basins: a reevaluation. Bulletin of the American Association of Petroleum Geologists 81, 1023–1041.

Parry, W.T., 1998. Fault-fluid compositions from fluid inclusion observations and solubilities of fracture-sealing minerals. Tectonophysics 290, 1–26.

Peacock, S.M., 1990. Fluid processes in subduction zones. Science 248, 329–337.

Ramsay, J.G., 1980. The crack-seal mechanism of rock deformation. Nature 284, 135–139.

Rice, J.R., Cleary, M.P., 1976. Some basic stress diffusion solutions for fluid-saturated elastic porous media with compressible constituents. Reviews of Geophysics and Space Physics 14, 227–241.

Robert, F., Brown, A.C., 1986. Archean gold-bearing quartz veins at the Sigma mine, Abitibi greenstone belt, Quebec: Part 1—Geologic relations and formation of the vein system. Economic Geology 81, 578–592.

Robert, F., Boullier, A.-M., Firdaous, K., 1995. Gold–quartz veins in metamorphic terranes and their bearing on the role of fluids in faulting. Journal of Geophysical Research 100, 12,861–12,879.

Roberts, R.G., 1987. Ore deposit models #1—Archean lode gold deposits. Geoscience Canada 14, 37–52.

Schaubs, P.M., Wilson, C.J.L., 2002. The relative roles of folding and faulting in controlling gold mineralization along the Deborah Anticline, Bendigo, Victoria, Australia. Economic Geology 97, 325–349.

Scholz, C.H., 1988. The brittle–plastic transition and the depth of seismic faulting. Geologische Rundschau 77, 319–328.

Secor, D.T., 1965. Role of fluid pressure in jointing. American Journal of Science 263, 633–646.

Seront, B., Wong, T.-F., Caine, J.S., Forster, C.B., Bruhn, R.L., Fredrich, J.T., 1998. Laboratory characterization of hydromechanical properties of a seismogenic normal fault system. Journal of Structural Geology 20, 865–882.

Seward, T.M., 1993. The hydrothermal geochemistry of gold. In: Foster, R.P., (Ed.), Gold Metallogeny and Exploration, Chapman and Hall, London, pp. 37–62.

Sibson, R.H., 1984. Roughness at the base of the seismogenic zone: contributing factors. Journal of Geophysical Research 89, 5791–5799.

Sibson, R.H., 1995. Selective fault reactivation during basin inversion: potential for fluid redistribution through fault-valve action. In: Buchanan, J.G., Buchanan, P.G. (Eds.), Basin Inversion. Geological Society Special Publication 88, pp. 3–19.

Sibson, R.H., 1996. Structural permeability of fluid-driven fault-fracture meshes. Journal of Structural Geology 18, 1031–1042.

Sibson, R.H., 1998. Brittle failure mode plots for compressional and extensional tectonic regimes. Journal of Structural Geology 20, 655–660.

Sibson, R.H., 2000. A brittle failure mode plot defining conditions for high-flux flow. Economic Geology 95, 41–48.

Sibson, R.H., Scott, J., 1998. Stress/fault controls on the containment and release of overpressured fluids: examples from gold–quartz vein systems in Juneau, Alaska, Victoria, Australia, and Otago, New Zealand. Ore Geology Reviews 13, 293–306.

Sibson, R.H., Robert, F., Poulsen, K.H., 1988. High-angle reverse faults, fluid-pressure cycling and mesothermal gold–quartz deposits. Geology 16, 551–555.

Terzaghi, K., 1943. Theoretical Soil Mechanics. John Wiley and Sons, New York.

Townend, J., Zoback, M.D., 2000. How faulting keeps the crust strong. Geology 28, 399–402.

Wilkinson, J.J., Johnston, J.D., 1996. Pressure fluctuations, phase separation, and gold precipitation during seismic fracture propagation. Geology 24, 395–398.

Williams, G.D., Powell, C.M., Cooper, M.A., 1989. Geometry and kinematics of inversion tectonics. In: Cooper, M.A., Williams, G.D. (Eds.), Inversion Tectonics. Geological Society Special Publication 44, pp. 3–15.

Zoback, M.D., Townend, J., 2001. Implications of hydrostatic pore pressures and high crustal strength for the deformation of intraplate lithosphere. Tectonophysics 336, 19–30.

Zoback, M.L., 1992. First- and second-order patterns of stress in the lithosphere: the World Stress Map project. Journal of Geophysical Research 97, 11,703–11,728.